An Investigative Study on the Effect of Various Parameters on Static and Dynamic Response of Hyperbolic Cooling Towers

Amritha Treesa
P G Student, Civil Engineering Department, FISAT, Angamaly, Kerala, India

Akshara S P
Assistant Professor, Civil Engineering Department, FISAT, Angamaly, Kerala, India

Abstract – Hyperbolic cooling towers are doubly curved cylindrical thin shell RC structures commonly used to provide cooling for large commercial buildings, industrial plants, steel mills etc. This paper discusses the static and dynamic response of two existing hyperbolic cooling towers of Bellary Thermal Station (BTPS) with varying height and thickness. ANSYS Workbench 16 is used for the analysis assuming top end free and bottom end fixed. These structures have been analyzed for self-weight, seismic loads and wind loads. Results are illustrated in graphical and tabular format. The improvement in structural performance based on stiffening rings is studied and a cooling tower with less liability to failure is suggested.

Index Terms – Hyperbolic cooling towers, Analysis, Stiffening rings.

1. INTRODUCTION

Hyperbolic cooling towers constitute are integral component of power generation systems and industrial plants which leads to environmental protection and reliability. The cooling towers, especially natural draft hyperbolic cooling towers are effectively used in thermal and nuclear power plants, chemical and petroleum industries and space conditioning processes.

Hyperbolic cooling towers are slender reinforced concrete structures having negative Gaussian curvature with doubly curved complex geometry. These structures are subjected to static and dynamic loads in which the membrane actions primarily resist the forces applied on the shells.

In natural draft hyperbolic cooling towers, moist air with low density inside the chimney in comparison with the dry and cool air outside the structure at same pressure makes the cooling process natural. The specially designed doubly curved Gaussian curvature of the structure provides superior stability against external pressures than straight towers. The wide base of the tower facilitates the evaporative cooling of the circulated water. The Narrowed throat of the tower stimulates the laminar flow of evaporation and diverging upper portion promotes turbulent mixing.

The whole shell structure is supported by diagonal, meridional, and vertical supporting columns. In order to achieve sufficient stability, cooling tower shells may be stiffened by additional rings both internally or externally as a repair or rehabilitation tool. The column supports can be of types A/V/X/Λ joined at the tower base or foundation level.

2. LITERATURE REVIEW

Collapse of a large-scale cooling tower under strong earthquakes was examined by Hongkui Ji [1]. The ground motion owing to the collapse was appropriately predicted using a comprehensive approach. The site geologies, typical hard soil with weathered sandy slate, moderate ground vibrations in the considered region can be various reasons for the collapse of the tower. Prediction of ground vibration due to the collapse of a 235 m high cooling tower under accidental loads was stated by Feng Lin [2].The study was based on accident loads such as wind and explosion. Various parameters were adopted for different collapse profiles, soil geologies and based on the arrangements of an isolation trench. It was found out that severe ground vibration may occur with increase in height. A new methodology for analysis of equivalent static wind loads on super large cooling towers was introduced by S T Ke [3]. A new method known as Consistent coupling method (CCM) was formulated for analyzing wind induced responses and corresponding equivalent static load. This method was found to be useful in determining background and resonant components using mode-acceleration method. The Optimum shape and design of cooling tower was examined by El Ansary [4]. A numerical tool based on coupling non-linear finite element model developed and a genetic algorithm optimization technique was used to find the optimum shape and design of the tower. Crosswinds effect on the performance of natural draft wet cooling towers was studied by Rafat Al-Waked [5]. The effect of crosswinds on cooling towers surrounded by power plant building structures was determined by a three-dimensional CFD model. It was stated as a vital tool to obtain qualitative results that can be implemented into parametric

studies. Finite element analysis of natural draught hyperbolic cooling tower by replacing columns by equivalent plate was formulated by A B Kulkarrni [6]. The study pointed that the either I or V column supports could be replaced by equivalent shell elements so that the analysis based on software become less tedious. The dynamics of axis symmetric hyperbolic shell structures was conducted by A M Nasir [7] to study the influence of curvature, wall thickness and shell height on vibration and dynamic response of the tower. It has been stated increase in curvature leads to decrease in time period first and then it is increased. It was also concluded that increase in height increases period of vibration.

3. MODELLING

Modelling was carried out in ANSYS workbench 16 software. Hyperbolic cooling towers existing at Bellary Thermal Power Station was modelled using finite element software. The cross section was drawn using lines and spline tools and the geometry of tower was generated by revolving the cross section. The static and dynamic loads were applied to the shells providing top end free and bottom end fixed.

3.1 Description of Geometry of Towers

Bellary thermal power station (BTPS) is a power generating unit located at Kudatini village in Bellary district, Karnataka. Two existing cooling towers as shown in Fig 1 & 2 were considered for the study. BTPS is situated at 15º11'58" N latitude and 76º43'23" E longitude.

Details of existing cooling towers

[1] The tower has a total height of 143.5 m. The base, throat and top radii are of 55 m, 30.5 m and 31.85 m respectively. The throat located 107.75 m above the base.

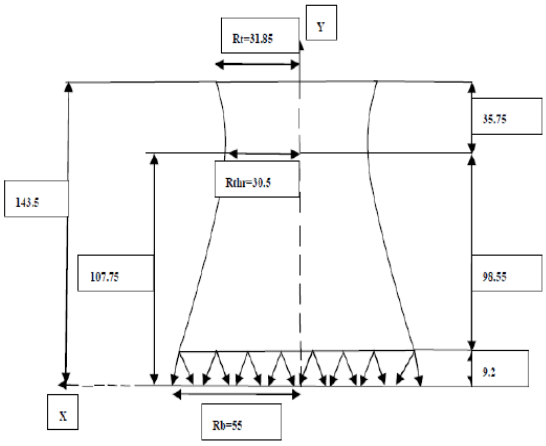

Figure 1 Geometry of existing cooling tower 1

[2] The tower has a total height of 175.5 m. The base, throat and top radii are 61 m, 34.375 m and 41.00m respectively. The throat located 131.60 m above the base.

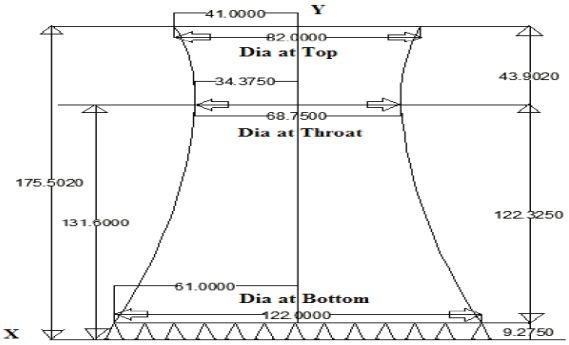

Figure 2 Geometry of existing cooling tower 2

CT1 & CT5 are existing cooling towers at BTPS .CT 2, CT 3, CT 4 are obtained by increasing the overall dimensions (height, base, throat and top diameter) of CT 1 by 5%, 10%, 15% without increasing the shell thickness of the tower as shown in table 1. The height was varied in order to find whether the increase in height of reference tower can have any influence on the response of the tower to static and dynamic loads.

Geometry description	CT1	CT2	CT3	CT4	CT5
Total height(m)	143.5	150.6	157.8	165.0	175.
Throat height(m)	107.7	113.1	118.5	123.1	131.
Top diameter (m)	63.6	66.78	69.96	73.14	82
Bottom diameter (m)	110	115.5	121	126.5	122
Throat diameter (m)	61	64.05	67.10	70.15	68.7
Column height	9.2	9.66	10.12	10.58	9.27

Table 1 Geometry descriptions

3.2 Finite Element Model

Considering the intricacy of the tower structure, material properties and the boundary conditions, finite element analysis is adopted. ANSYS Workbench 16 is used for the finite element analysis providing fixity at bottom end and considering top end free. A typical finite element model of tower is shown in Fig. 3

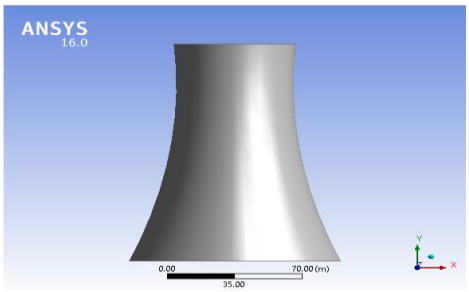

Figure 3 Finite element model of CT1

3.3 Material Properties for the Analysis

The material properties assumed for the analysis of the tower are as follows:

- Young's modulus: - 31Gpa.
- Poisson's Ratio: - 0.15.
- Density of RCC: - 25 kN/m^3.

4. FINITE ELEMENT ANALYSIS RESULTS

Analysis of the towers can be done in finite element software ANSYS Workbench 16 .Various analysis were carried out like Static Analysis, Modal Analysis, Buckling Analysis ,Wind Analysis and Transient Analysis

4.1 Static Analysis

The actual thickness of existing cooling towers CT1 and CT5 are 200mm. Static Structural Analysis were carried out for all the towers by varying the thickness (i.e. 200mm,250mm,300mm,350mm,400mm,450mm,500mm)to find out the total deformation, Von-Misses Stress, and Maximum Principal Stress. The results are tabulated in table 2.

Model	Thickness (mm)	Total Deformation (mm)	Equivalent Stress(MPa)	Max. Principal Stress(MPa)
CT1	200	6.347	2.6493	0.064721
	250	5.0772	2.1458	0.051753
	300	4.2308	1.8054	0.043115
	350	3.5704	1.5505	0.038859
	400	3.1239	1.3653	0.033989
	450	2.7767	1.2201	0.030204
	500	2.4989	1.1031	0.027176
CT2	200	6.9667	2.7833	0.0607
	250	5.5731	2.2526	0.048547
	300	4.644	1.894	0.04044
	350	3.9804	1.6351	0.03466
	400	3.4827	1.4392	0.03032
	450	3.0956	1.2856	0.026955
	500	2.7859	1.162	0.024259
CT3	200	7.6801	2.9498	0.071309
	250	6.1437	2.3878	0.057028
	300	5.1194	2.008	0.047513
	350	4.3878	1.7337	0.04072
	400	3.8392	1.526	0.035628
	450	3.4124	1.3633	0.031669

	500	3.071	1.2322	0.028502
CT4	200	8.4962	3.161	0.09535
	250	6.7964	2.5608	0.076267
	300	5.6632	2.1546	0.063547
	350	4.8538	1.8609	0.054466
	400	4.2467	1.6385	0.047656
	450	3.7746	1.4641	0.042362
	500	3.3969	1.3235	0.038127
CT5	200	10.003	3.3593	0.2265
	250	8.0019	2.7184	0.18108
	300	6.6617	2.2853	0.15082
	350	5.7148	1.9724	0.12921
	400	5.0001	1.7357	0.113
	450	4.4442	1.5502	0.1004
	500	3.9996	1.4008	0.090321

Table 2 Static analysis results

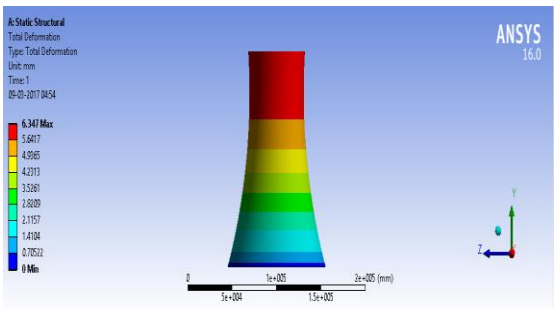

Figure 4 Total deformations (CT1 200mm)

The sample pattern of total deformation, equivalent stress and maximum principal stress (CT1 200mm thickness) were illustrated in Fig.4, Fig.5& Fig 6.

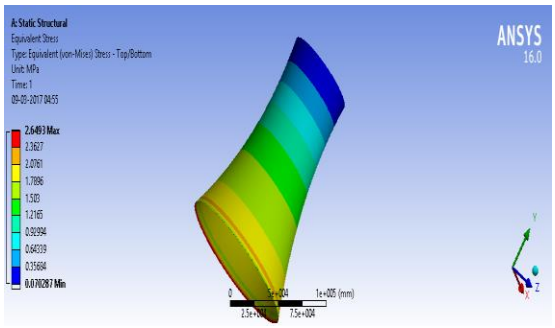

Figure 5 Equivalent stress (CT1 200mm)

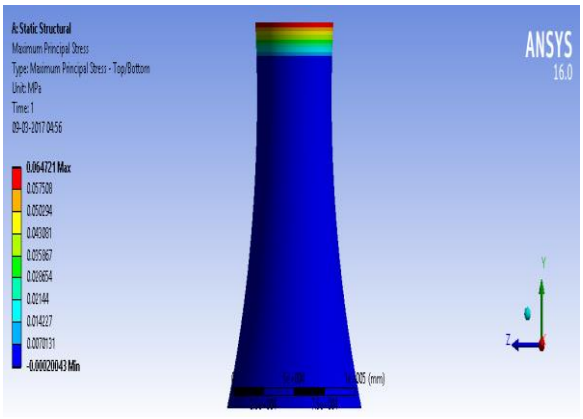

Figure 6 Maximum Principal Stress (CT1 200mm)

The variation of total deformation, Equivalent stress and maximum principal stress with varying height and thickness were shown in Fig. 7 to 13.

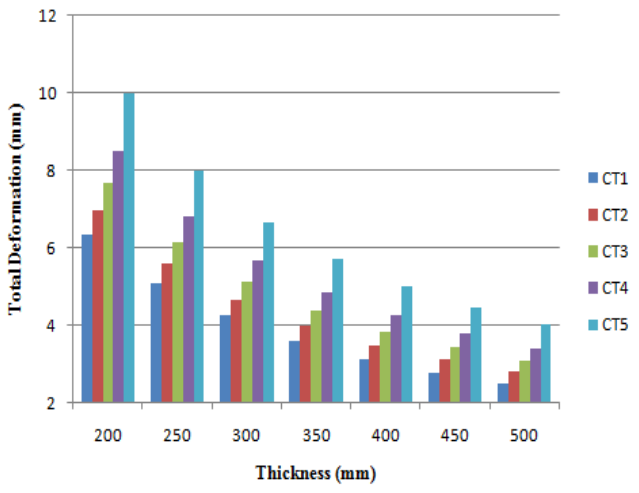

Figure 7 Variation of total deformation with thickness (for all towers for a specified thickness)

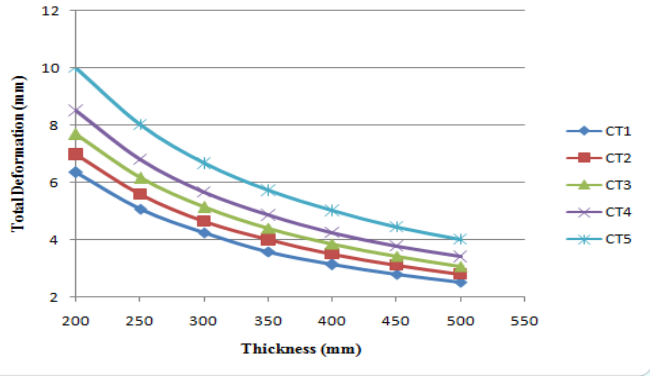

Figure 8 Variation of total deformation with thickness (for a particular tower for a specified thickness)

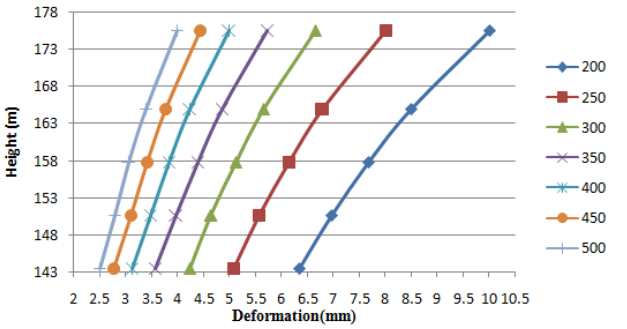

Figure 9 Variation of total deformation with height

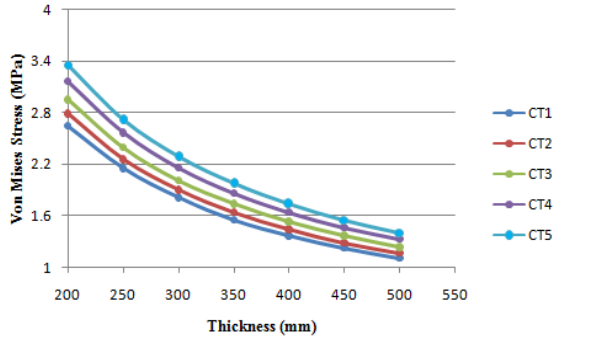

Figure 10 Variation of Von mises stress with thickness

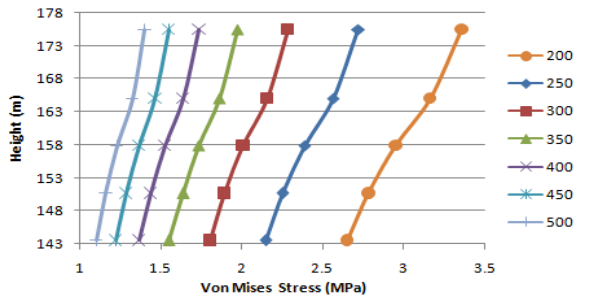

Figure 11 Variation of Von mises stress with height

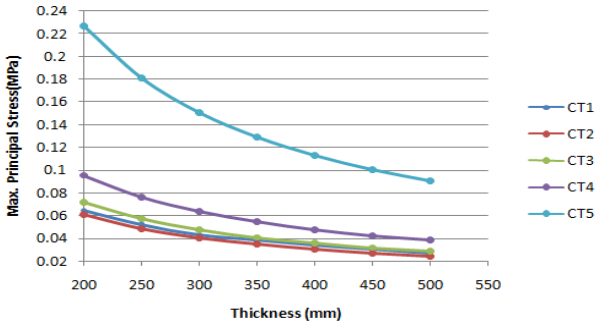

Figure 12 Variation of maximum principal stress with thickness

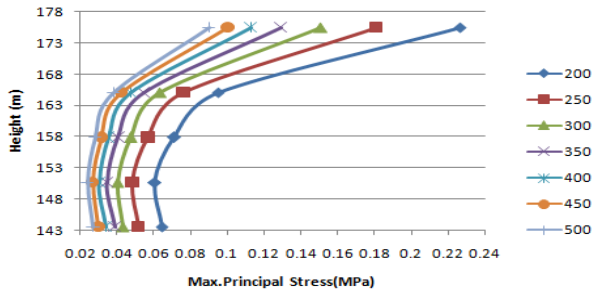

Figure 13 Variation of maximum principal stress with height

4.2 Modal Analysis

The modal analysis is carried out to calculate the natural frequency and the deformation at different modes. The results are tabulated in Table 3.

Model	Thickness (mm)	Frequency (Hz)		
		1 Mode	5 Mode	10 Mode
CT1	200	1.0929	1.1833	1.2678
	250	1..202	1.2897	1.4255
	300	1.2235	1.3847	1.4531
	350	1.2598	1.4567	1.6247
	400	1.2875	1.4596	1.6971

	450	1.3182	1.5126	1.719
	500	1.3154	1.6066	1.7445
CT2	200	1.0233	1.0982	1.1685
	250	1.0816	1.1698	1.3063
	300	1.1328	1.2646	1.3545
	350	1.1542	1.3328	1.46
	400	1.1782	1.3597	1.5937
	450	1.204	1.3772	1.613
	500	1.2336	1.4608	1.6342
CT3	200	0.9733	1.0703	1.1152
	250	1.0256	1.1062	1.2289
	300	1.0848	1.2217	1.3028
	350	1.1201	1.2843	1.3751
	400	1.1415	1.3074	1.5067
	450	1.11652	1.3101	1.5243
	500	1.1909	1.37	1.5435
CT4	200	0.93853	1.055	1.1075
	250	0.9874	1.0936	1.1753
	300	1.0428	1.2076	1.271
	350	1.1037	1.273	1.3399
	400	1.14	1.275	1.4202
	450	1.16	1.2799	1.4373
	500	1.19	1.3115	1.4968
CT5	200	0.8970	1.0093	1.0674
	250	0.94625	1.0795	1.1383
	300	1.0016	1.1578	1.826
	350	1	1.1598	1.2461
	400	1.1217	1.1621	1.3166
	450	1.148	1.1966	1.3935
	500	1.1675	1.2686	1.4742

Table 3 Modal analysis results

The sample pattern of total deformation for mode 1, 5 & 10 (CT1 200mm thickness with mass participation factor=1) were illustrated in Fig.14, Fig.15& Fig. 16.

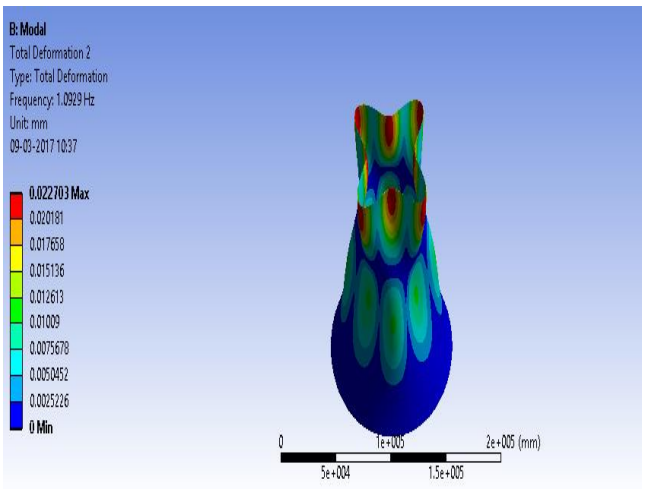

Figure 14 Total deformations for mode1 (200mm CT1)

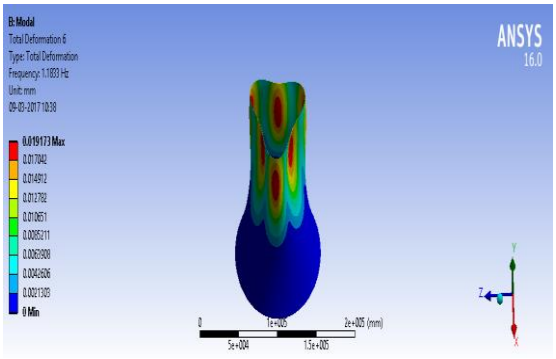

Figure 15 Total deformation for mode 5 (200mm CT1)

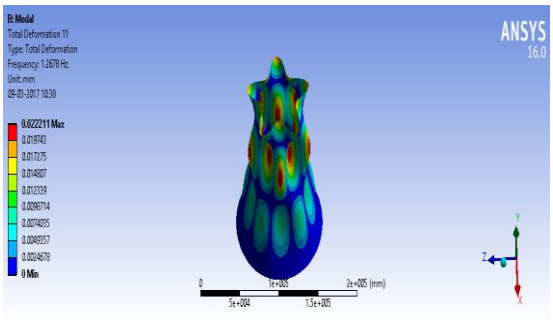

Figure 16 Total deformation for mode 10 (200mm CT1)

The variation of frequency with varying height and thickness for modes 1, 5, 10 were shown in Fig. 17 to 19.

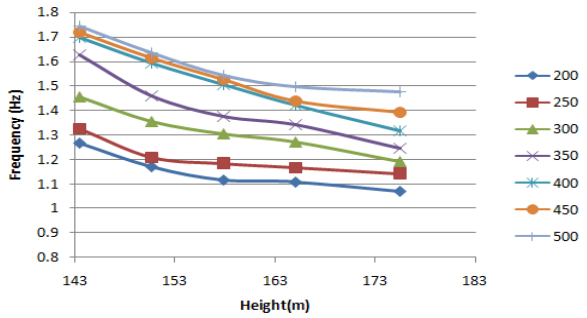

Figure 17 Variation of frequency with height (mode1)

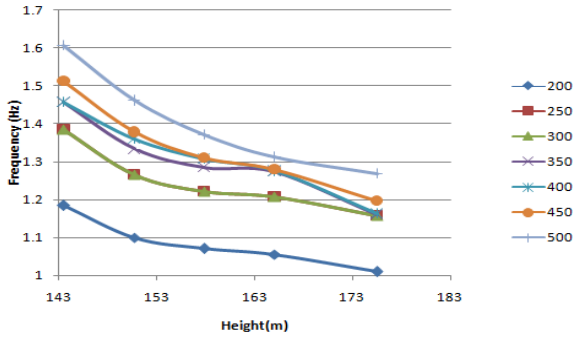

Figure 18 Variation of frequency with height (mode5)

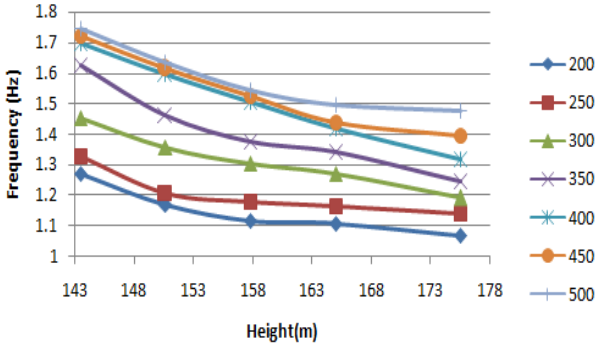

Figure 19 Variation of frequency with height (mode10)

4.3 Buckling Analysis

Buckling analysis was carried out for all the cooling towers by varying the thickness and the total deformation corresponding 1, 3, 5 modes (mass participation factor =1) were calculated. The results are tabulated in table 4.

Model	Thickness	Total deformation(mm)			Critical buckling load, N/mm^2
		1	3	5	
CT1	200	1.053	1.061	1.062	0.043
	250	1.055	1.063	1.064	0.076
	300	1.056	1.064	1.066	0.116
	350	1.057	1.067	1.068	0.169
	400	1.058	1.068	1.070	0.229
	450	1.059	1.07	1.072	0.305
	500	1.063	1.071	1.075	0.392
CT2	200	1.055	1.063	1.064	0.039
	250	1.056	1.064	1.065	0.068
	300	1.058	1.066	1.067	0.104
	350	1.059	1.067	1.071	0.152
	400	1.063	1.069	1.072	0.203
	450	1.064	1.070	1.075	0.271
	500	1.069	1.072	1.077	0.352

CT3	200	1.057	1.064	1.066	0.034
	250	1.058	1.066	1.067	0.060
	300	1.062	1.069	1.07	0.092
	350	1.064	1.071	1.072	0.134
	400	1.069	1.072	1.073	0.183
	450	1.071	1.075	1.078	0.240
	500	1.077	1.078	1.08	0.310
CT4	200	1.06	1.065	1.067	0.30
	250	1.064	1.068	1.069	0.052
	300	1.069	1.071	1.072	0.082
	350	1.073	1.074	1.073	0.118
	400	1.074	1.075	1.076	0.164
	450	1.076	1.078	1.08	0.213
	500	1.081	1.082	1.083	0.272
CT5	200	1.063	1.066	1.068	0.029
	250	1.067	1.068	1.069	0.05
	300	1.070	1.072	1.073	0.089
	350	1.075	1.076	1.075	0.128
	400	1.077	1.078	1.079	0.169
	450	1.081	1.082	1.083	0.213
	500	1.085	1.086	1.088	0.271

Table 4 Buckling analysis results

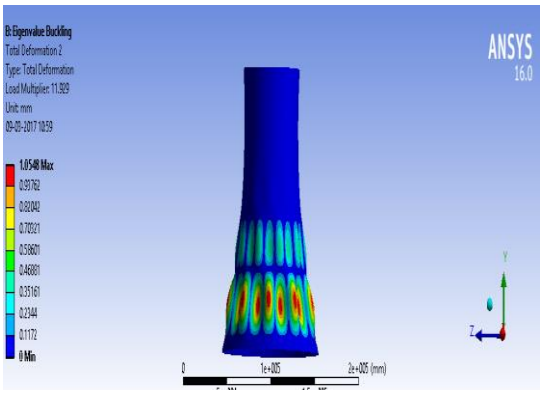

Figure 20 Total deformation for mode 1(CT1 200mm)

The sample pattern of total deformation for mode 1, 3 & 5 (CT1 200mm thickness with mass participation factor=1) were illustrated in Fig.20, Fig.21& Fig. 22.

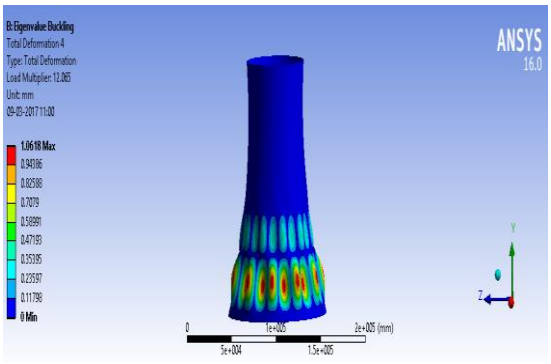

Figure 21 Total deformation for mode 3(CT1 200mm)

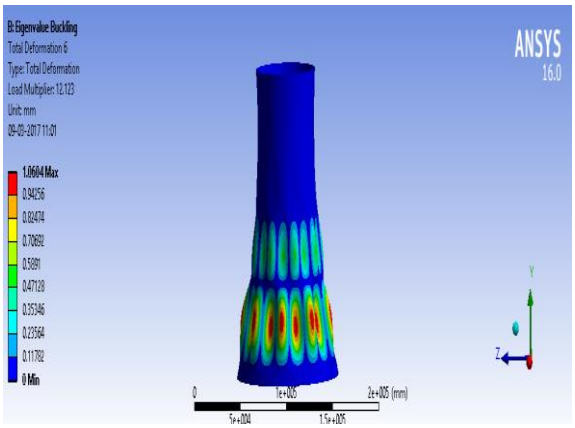

Figure 22 Total deformation for mode 5(CT1 200mm)

The variation of total deformation with varying height and thickness for modes 1, 3, 5 were shown in Fig. 23 to 25.

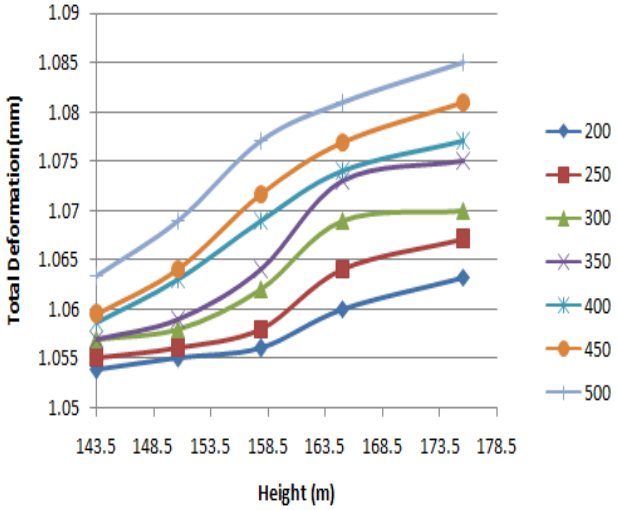

Figure 23 Variation of total deformation with height (mode 1)

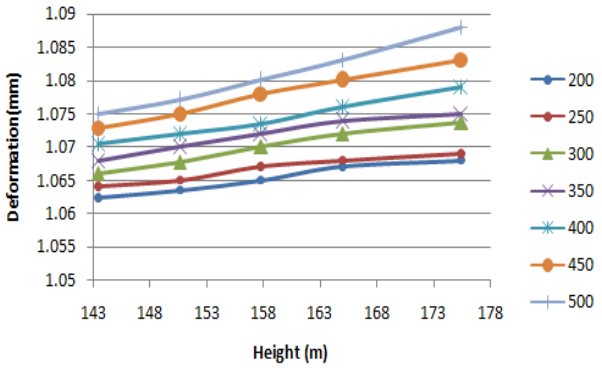

Figure 24 Variation of total deformation with height (mode 3)

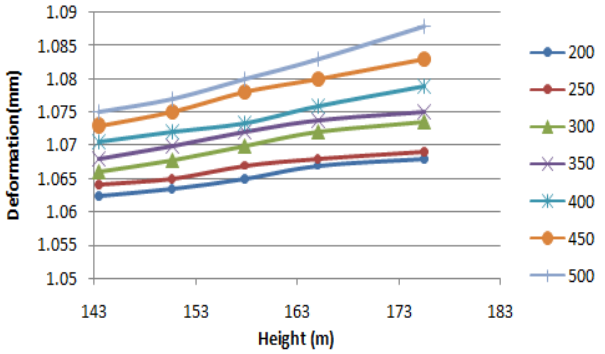

Figure 25 Variation of total deformation with height (mode 5)

4.4 Wind Analysis

The wind analysis is carried out by providing wind load in x and z directions to find out the total deformation and the stress caused by the wind loads at the topmost portion (for Θ=0° & Θ=70°).The results (Θ=0°) were tabulated in table 5 and for (Θ=70°) in table 6.

Model	Thickness	Total Deformation(mm)	Equivalent stress (MPa)	Max.Principal Stress(MPa)
CT1	200	42.407	5.998	5.877
	250	33.928	4.853	4.7705
	300	28.276	4.0828	4.0228
	350	23.527	3.494	3.445
	400	20.587	3.079	3.041
	450	18.301	2.7543	2.7247
	500	16.472	2.4929	2.4693
CT2	200	46.386	6.395	6.273
	250	37.112	5.175	5.092
	300	30.929	4.3541	4.2937
	350	26.512	3.7622	3.717
	400	23.2	3.3151	3.2804
	450	20.623	2.9651	2.9381
	500	18.562	2.6835	2.662
CT3	200	51.31	6.638	6.51
	250	41.051	5.369	5.2
	300	34.211	4.5144	4.457
	350	29.326	3.898	3.856
	400	25.662	3.434	3.4023
	450	22.812	3.0706	3.0462
	500	20.532	2.7781	2.7593
CT4	200	57.363	6.761	6.655
	250	45.894	5.461	5.3917
	300	38.248	4.586	4.539
	350	32.786	3.9577	3.9244
	400	28.69	3.483	3.4594
	450	25.50	3.1121	3.0952
	500	22.955	2.8139	2.802
CT5	200	84.045	7.81	7.875

	250	67.24	6.2907	6.3547
	300	56.036	5.2717	5.333
	350	48.033	4.5403	4.5984
	400	42.031	3.9894	4.044
	450	37.363	3.559	3.6114
	500	33.628	3.212	3.2636

Table 5 Wind analysis results (Θ=0°)

The wind analysis results for (Θ=70°) is tabulated below in table 6

Model	Thickness	Total Deformation (mm)	Equivalent stress(MPa)	Max.Principal Stress(MPa)
CT1	200	44.334	6.271	6.1445
	250	35.47	5.0742	4.9874
	300	29.561	4.2683	4.2056
	350	24.569	3.653	3.6023
	400	21.523	3.2191	3.1798
	450	19.133	2.8794	2.8485
	500	17.221	2.6062	2.5815
CT2	200	48.494	6.6861	6.5587
	250	38.789	5.4109	5.3235
	300	32.334	4.552	4.4888
	350	27.717	3.932	3.8859
	400	24.254	3.4657	3.4295
	450	21.561	3.0998	3.0716
	500	19.406	2.8055	2.7832
CT3	200	53.641	6.9404	6.816
	250	42.916	5.6131	5.5289
	300	35.766	4.7195	4.6595
	350	30.659	4.0761	4.0319
	400	26.828	3.5903	3.5569
	450	23.849	3.2101	3.1846
	500	21.465	2.904	2.8847
CT4	200	59.97	7.069	6.9577
	250	47.98	5.7093	5.6367
	300	39.986	4.7951	4.7455
	350	34.276	4.1375	4.1027
	400	29.994	3.6414	3.6167
	450	26.663	3.2535	3.2359
	500	23.998	2.9418	2.9294
CT5	200	87.864	8.1649	8.7411
	250	70.295	6.5766	6.6435
	300	58.583	5.5113	5.7554
	350	50.216	4.7466	4.8074
	400	43.941	4.1707	4.2282
	450	39.061	3.7211	3.7755
	500	35.156	3.3603	3.4119

Table 6 Wind analysis results (Θ=70°)

The sample pattern of total deformation, equivalent stress and maximum principal stress were illustrated in Fig.26, Fig.27& Fig 28.

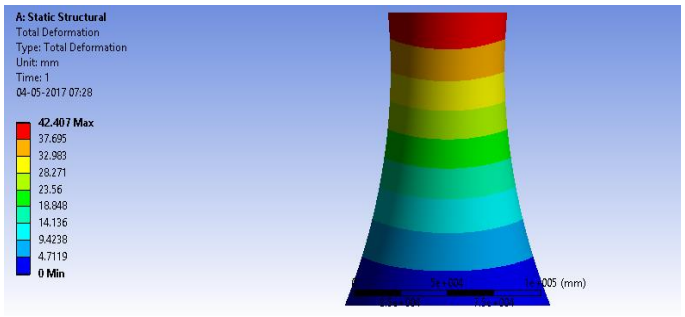

Figure 26 Pattern of total deformation

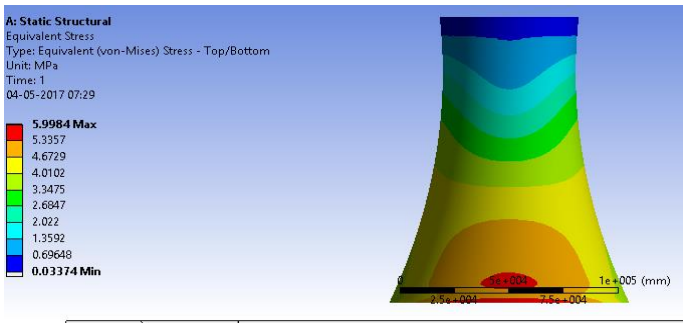

Figure 27 Pattern of Equivalent stress

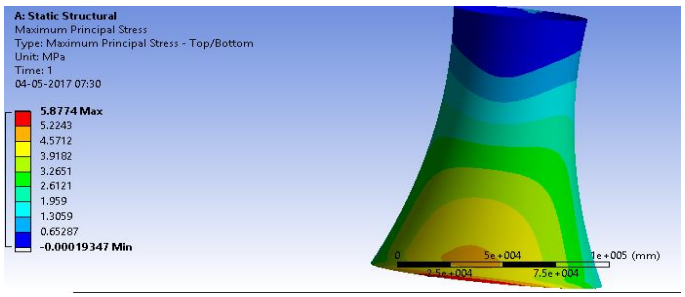

Figure 28 Pattern of maximum principal stress

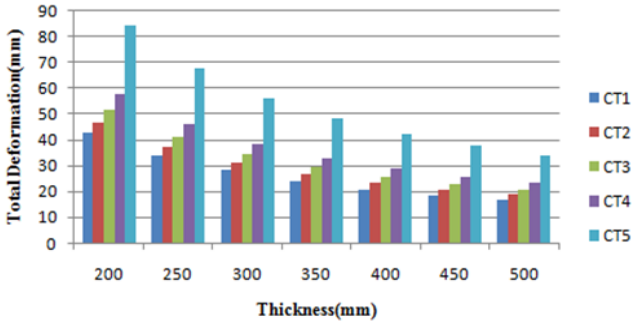

Figure 29 Variation of total deformation with thickness (for all towers for a specified thickness)

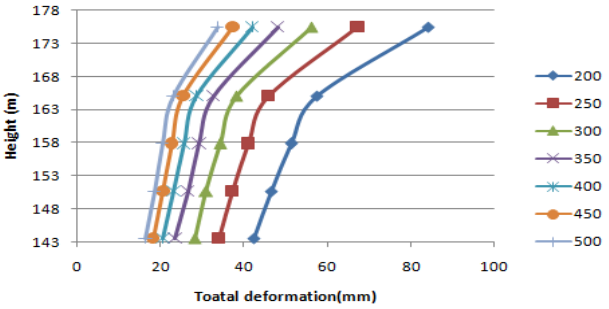

Figure 30 Variation of total deformation with height

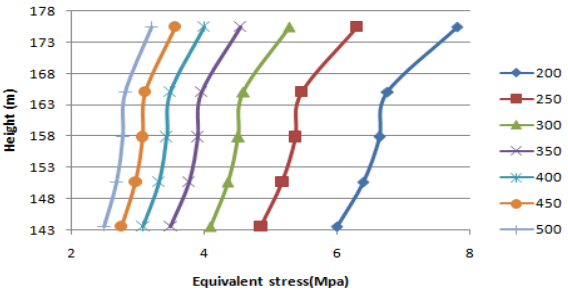

Figure 31 Variation of equivalent stress with height

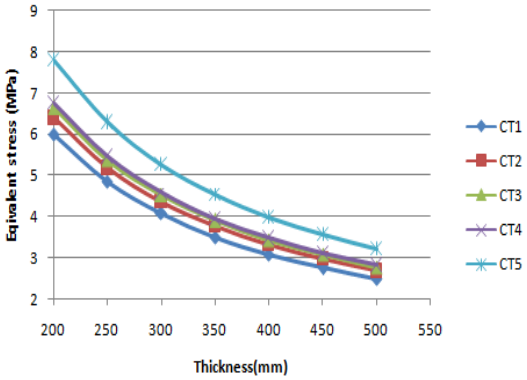

Figure 32 Variation of equivalent stress with thickness

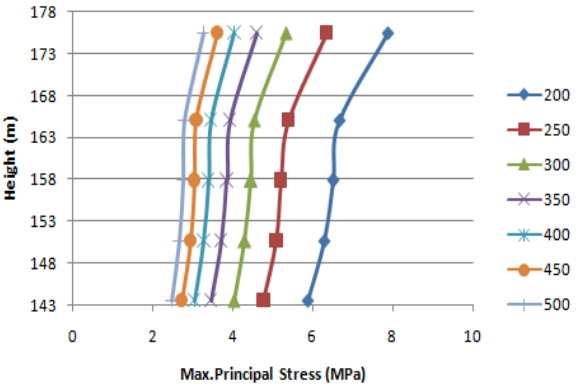

Figure 33 Variation of maximum principal stress with height

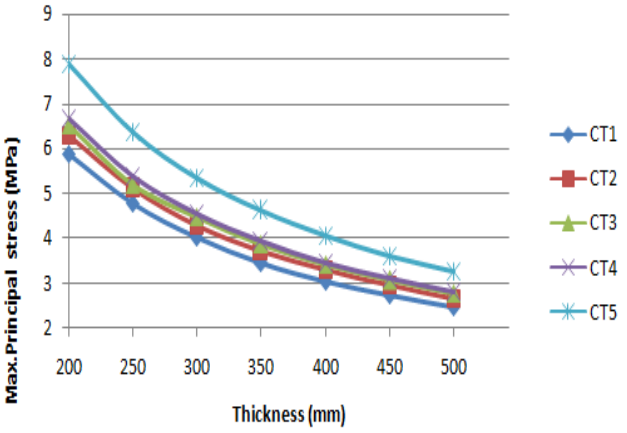

Figure 34 Variation of maximum principal stress with thickness

For Θ= 70°:-

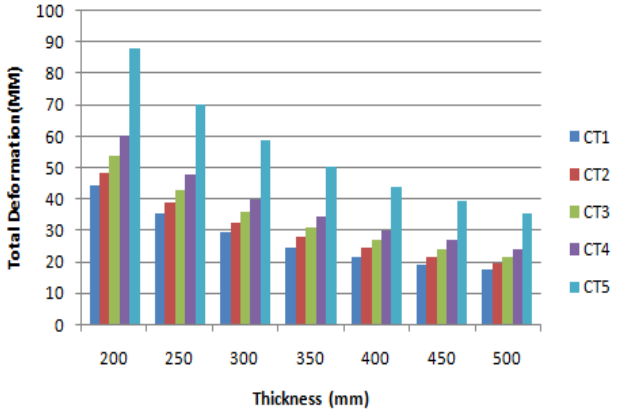

Figure 35 Variation of total deformation with thickness (for all towers for a specified thickness)

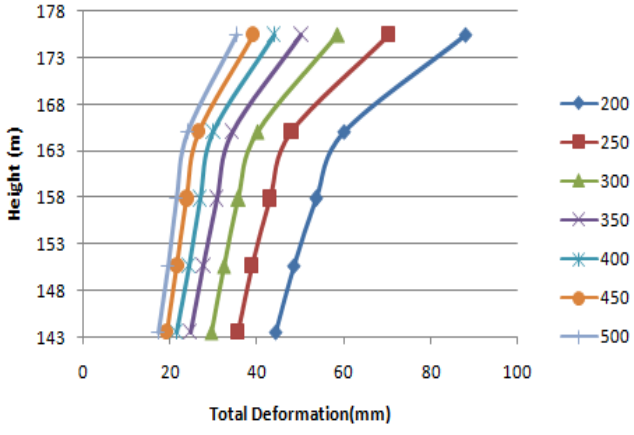

Figure 36 Variation of total deformation with height

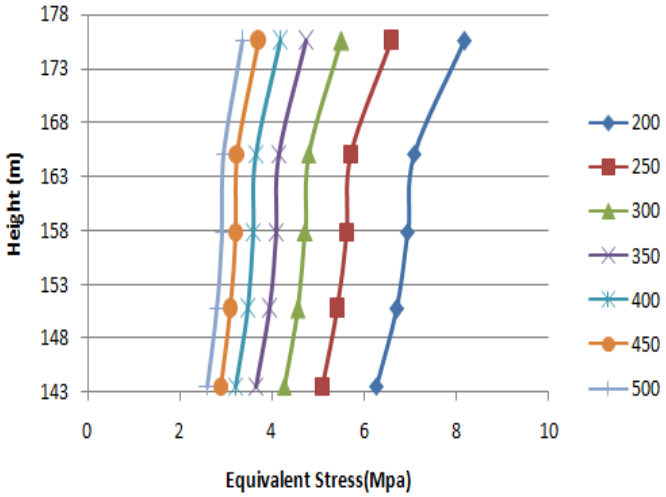

Figure 37 Variation of equivalent stress with height

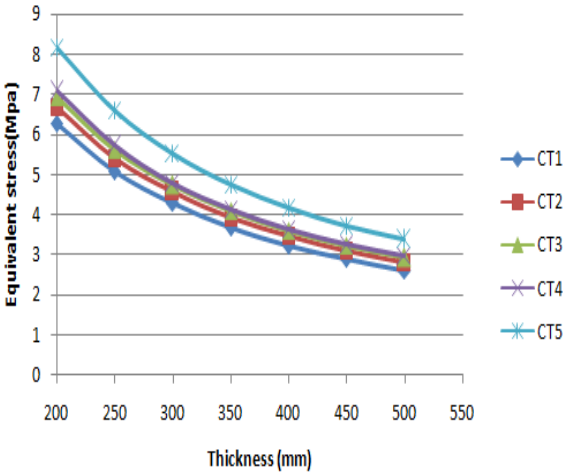

Figure 38 Variation of equivalent stress with thickness

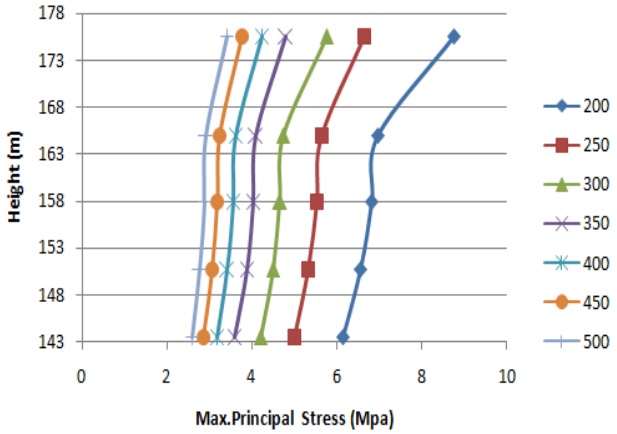

Figure 39 Variation of maximum principal stress with height

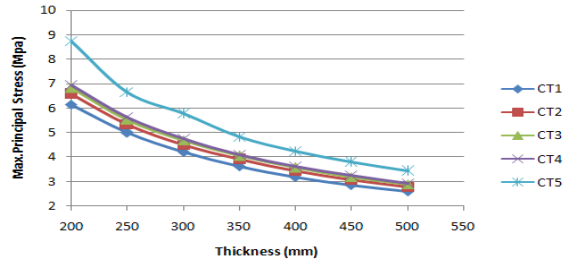

Figure 40 Variation of maximum principal stress with thickness

4.4 Transient Analysis

Transient dynamic analysis is a technique used to determine the dynamic response of a structure under the action of any general time-dependent loads. The transient analysis was conducted for all the towers for 200mm thickness. Since seismic effect is minimum in cooling tower compared to wind effect time history plot was studied only for the existing towers CT1 and CT5.The results are tabulated in table 7.

The data for time history analysis is provided as obtained from 1994 Northridge earthquake occurred on January 17, at 4:30:55 a.m.

Model	Total Deformation (mm)	Directional Deformation (mm)	Equivalent stress (MPa)	Maximum Principal Stress(MPa)
CT1	6.3452	5.789	2.6523	0.06
CT2	6.9649	6.5921	2.7868	0.0607
CT3	7.6784	7.23	2.9541	0.071303
CT4	8.494	8.142	3.167	0.95353
CT5	10. 36	10.138	3.365	0.22654

Table 7 Transient analysis results

The time history graph obtained from transient analysis of CT1 and CT5 are shown in figures 41 to 42.

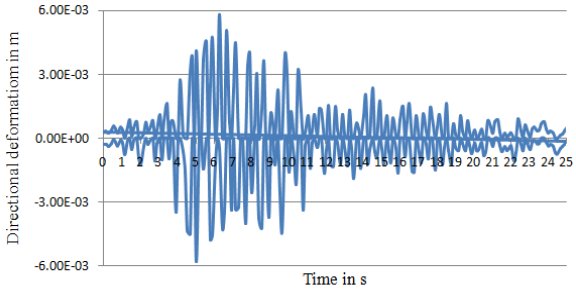

Figure 41 Time history for CT1

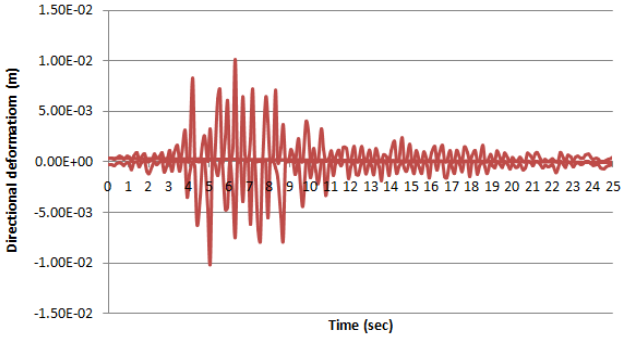

Figure 42 Time history for CT5

5. EFFECT OF STIFFENING RINGS AS A METHOD OF RECTIFICATION

To increase the R.C. hyperbolic cooling towers structural stability while keeping the costs down, engineers could add stiffening rings. To achieve maximum buckling stability, important design parameters such as the number, dimension, and location of stiffening rings must be considered.

The existing cooling tower CT5 of 200mm thickness has maximum deformation in all the analysis. In order to improve its performance, a stiffener ring is proposed.

5.1 Effect of Stiffener Ring Location

For improving the buckling stability of the R.C. hyperbolic cooling tower, several configurations were created by adding an additional stiffening ring to structure. The stiffener width and height is chosen as per the codal provisions (ie. 2 to 7 times the thickness).For the time being a stiffener of 400mmx1000mm is taken for the study. The stiffener was placed at different locations along the height of the tower and the Bucking Safety Factor (BSF) was determined. The results obtained by placing the stiffener ring at various locations are shown in table 8.

Sl. No	Height(m)	BSF
1	15	8.013
2	30	8.12
3	45	8.29
4	60	8.56
5	65	8.731
6	75	8.69

7	90	8.296
8	105	8.2
9	120	8.15
10	135	8.09
11	150	8
12	165	7.95
13	175	7.93

Table 8 Effect of stiffener ring location

The result is represented in graphical format in figure 43.From the graph we could notice that the maximum BSF is at 65m.Hence stiffener of 400mmx1000mm has to be placed at 65m in order to provide buckling stability.

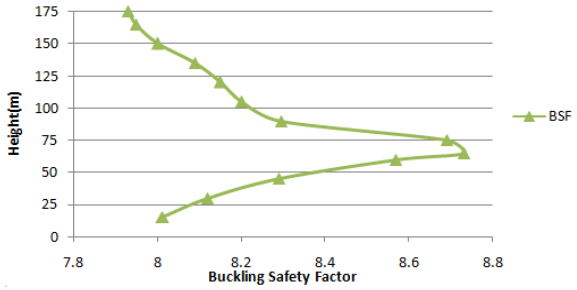

Figure 43 Effect of stiffener ring location on BSF

5.2 Effect of Stiffener Thickness

The first set-up (with one stiffening ring at 65 m) was used to examine the effect of the stiffening ring thickness on the BSF of R.C. hyperbolic cooling towers. The thickness was considered to vary in the range from 100 to 1000 mm. The width of the stiffening ring remained a constant value (1000 mm).The same procedure is repeated using two and three stiffening rings. The results obtained from the study are given in table 9 and were illustrated in figure 44.

Thickness	Buckling Safety Factor(BSF)		
	One stiffening ring	Two stiffening ring	Three stiffening ring
0.2	8.418	8.449	8.4954
0.4	8.73	8.9215	8.93
0.6	8.8595	8.99	9.01
0.8	8.865	9.0468	9.08
1	8.87	9.0918	9.16
1.2	8.89	9.139	9.19

Table 9 BSF as a function of stiffener thickness

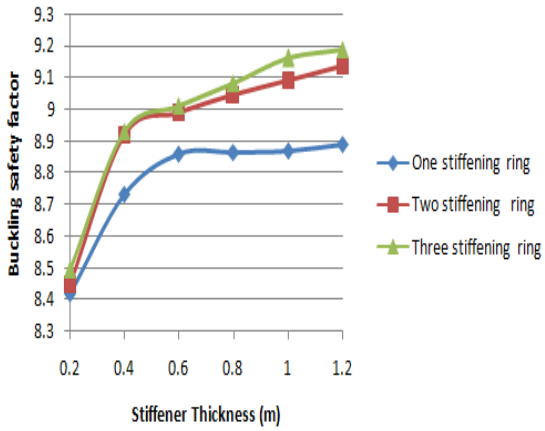

Figure 44 BSF as a function of stiffener ring thickness

5.3 Effect of Stiffener Width

The first set-up (with one stiffening ring at 65 m) was used to examine the effect of the stiffening ring width on the BSF of R.C. hyperbolic cooling towers. the stiffening width was considered to vary in the range from 500 to 1500 mm. The thickness of the stiffening ring remained a constant value (600 mm).The results obtained are presented in table 10 and are illustrated in figure 45.

Width(m)	Buckling Safety Factor(BSF)		
	One Stiffening Ring	Two Stiffening Ring	Three Stiffening Ring
0.5	8.521	8.5346	8.5725
0.75	8.68	8.84	8.89
1	8.731	8.89	8.94
1.25	8.738	8.942	8.951
1.5	8.752	8.949	8.953

Table 10 BSF as a function of stiffener ring width

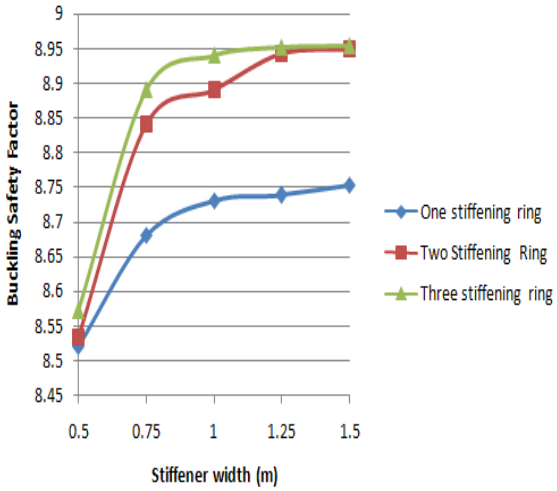

Figure 45 BSF as a function of stiffener ring width

5.4 Effect of Stiffener Ring on Wind Effect

In order to reduce the deformation due to wind load, an alternate technique for the rectification is to provide stiffeners at various locations of the hyperbolic cooling tower. Since on examining the five cooling towers, we could find that maximum deformation at sideward and windward direction occur for CT5of 200mm thickness. Hence stiffener has to be placed at different location of CT5. One stiffener ring of 60mmx1200mm is provided at all locations and the deformation obtained is tabulated in table 11 and are illustrated in figure 47& 48.

Sl. No	Location	Total Rings	Deformation (mm)	Equivalent Stress(Mpa)
1	Throat[3] &Top[1]	2	76.95	6.9
2	Throat[3]& Bottom[5]	2	85.691	7.65
3	Throat [3]& Centre Upper[2]	2	80.98	7.176
4	Throat[3] & Centre Bottom[4]	2	81.62	7.523
5	Throat[3], Top[1] & Bottom[5]	3	79.82	7.068
6	Throat[3], Top[1] & Centre Upper[2]	3	78.078	7.057
7	Throat[3], Top [1]& Centre Bottom[4]	3	81.26	7.3844
8	Throat[3], Bottom [5]& Centre Upper[2]	3	80.07	7.143
9	Throat[3], Bottom[5]& Centre Bottom[4]	3	82.97	7.32
10	Throat[3], Top[1], Bottom[5] & Centre Upper[2]	4	64.57	5.803
11	Throat[3], Top[1], Bottom[5] & Centre Bottom[4]	4	64.63	5.823
12	At all locations	5	62.543	5.623

Table 11 Location of stiffeners and results

The different locations were stiffening ring provided is shown in figure 46.

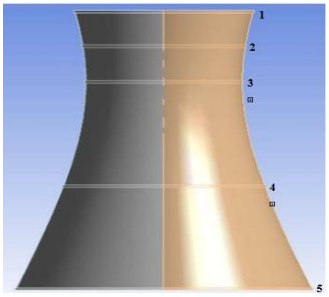

Figure 46 Stiffener ring location

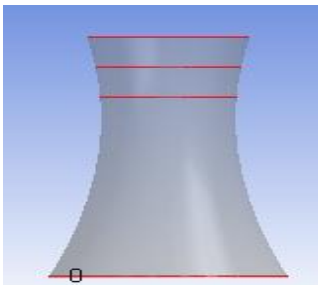

Figure 47 Throats, Top, Bottom & Centre Upper

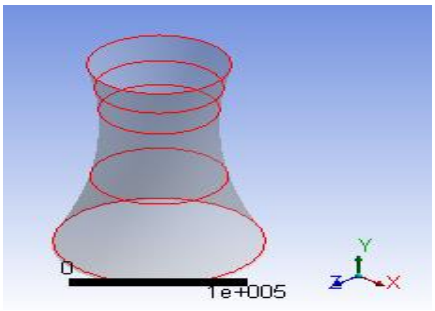

Figure 48 At all locations

Further analysis was repeated for CT5 with 200mm thickness by using two stiffener rings of 600mmx1200mm at the same locations were one stiffener ring was provided. The results obtained are shown in table 12 and are illustrated in figure 49& 50.

Sl. No	Location	Total Rings	Deformation (mm)	Equivalent Stress(Mpa)
1	Throat[3] &Top[1]	4	64.49	5.866
2	Throat[3]& Bottom[5]	4	77.402	6.9822
3	Throat [3]& Centre Upper[2]	4	67.245	6.0504
4	Throat[3] & Centre Bottom[4]	4	73.987	6.657
5	Throat[3], Top[1] & Bottom[5]	6	67.18	5.96
6	Throat[3], Top[1] & Centre Upper[2]	6	64.652	5.865
7	Throat[3], Top [1]& Centre Bottom[4]	6	64.793	6.05
8	Throat[3], Bottom [5]& Centre Upper[2]	6	65.194	5.865
9	Throat[3], Bottom[5]& Centre Bottom[4]	6	67.25	6.39
10	Throat[3], Top[1], Bottom[5] & Centre Upper[2]	8	60.25	5.61
11	Throat[3], Top[1], Bottom[5] & Centre Bottom[4]	8	61.3	5.76
12	At all locations	10	59.84	5.575

Table 12 Location of two stiffeners and results

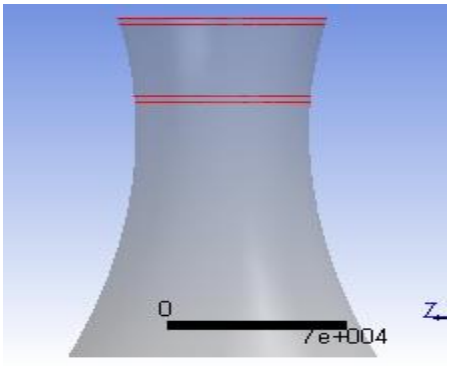

Figure 49 Two stiffener rings at top and throat

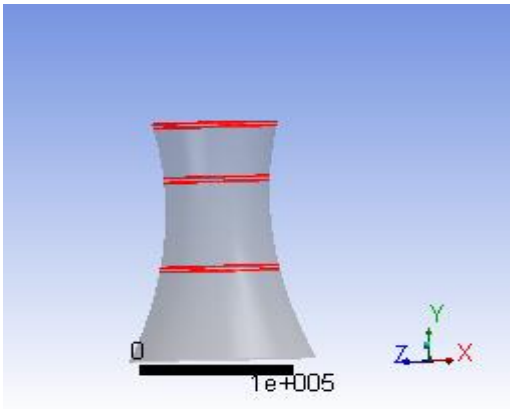

Figure 50 Two stiffener rings at top, throat and central bottom

6. CONCLUSIONS

The following conclusions are made from the study conducted,

- Static and wind analysis (Θ=0° and Θ= 70°) were conducted. The inferences obtained from the analysis are as follows

  As the height increases for a particular thickness, total deformation increases. It can also be seen that as thickness increases total deformation decreases. As height increases deformation for a particular thickness increases.

  The equivalent stress decreases with increase in thickness. At the same time it increases with increase in height for a particular thickness.

  The maximum principal stress decreases with increase in thickness. As height increases for a specified thickness maximum principal stress decreases.

- Modal analysis was conducted to study the vibration characteristics of cooling towers. It can be seen that for a particular thickness, as height increases, frequency decreases.

- From buckling analysis, it was clear that as the height increases deformation increases for a particular thickness. As the height increases the critical buckling load decreases leading to buckling instability. The critical load of CT5 IS 32.5% less compared to CT1.

- In wind analysis maximum deformation is obtained for CT5 at 200mm thickness (84 mm at Θ=0° and 87mm at Θ=70°).The permissible deformation as per the code of hyperbolic cooling tower is 90 mm. And the corresponding equivalent stresses are 7.81MPa and 8.16 MPa. The permissible stress for M30 concrete is 10 N/mm^2 in bending and $8N/mm^2$ in direct compression. Since the values obtained is about to limit proper rectification methods should be provided for CT5.

- On transient analysis done as per the data of north ridge earthquake it is seen that maximum directional deformation occurs at 6 seconds and minimum directional deformation occurs at 5 seconds. The results obtained for transient analysis is almost same as that of static analysis.

- On comparing the deformations and stresses induced on the structure by wind and seismic loads it is clear that the wind load is dominant in a hyperbolic cooling tower than seismic loads.

- In order to rectify the stability issues and the large deformations caused by wind, two stiffener of 600mmx1200mm were provided

- It was found out that the buckling stability can be obtained by using two stiffeners of 600x1200mm at a height of about 65m from the base.

- The deformation corresponding to wind should have a permissible limit of 90 mm. And it was seen that the deformation and stresses induced on CT5 was near to 90mmand 10 N/mm^2 for 200mm thickness. Hence stiffeners have to be provided at different levels for improving the performance.

- Providing one stiffener ring of 600mmx1200 mm either at top, throat, bottom, central upper or two stiffener rings of 600mmx1200mm at top and throat portion or top, throat and central bottom portion can reduce the deformation and stresses to a desirable limit.

- Hence from the above analysis conducted, it can be concluded that hyperbolic cooling tower at a height almost to about 170 m with proper stiffener ring at proper locations can increase the efficiency of the cooling tower. Since the seismic load is less dominant in hyperbolic cooling towers increase in height will not cause the structures failure instead it increases the cooling efficiency.

REFERENCES

[1] Hongkui Ji**, "**Prediction of ground motion due to the collapse of large-scale cooling tower under strong earthquakes", Soil Dynamics and Earthquake engineering, Vol.65, pp .43-54. 2014.

[2] Feng Lin et.al, "prediction of ground vibration due to the collapse of a 235 m high cooling tower under accidental loads", Soil Dynamics and Earthquake engineering ,Vol.65 ,pp .43-54, 2013.

[3] S.T. Ke, Y.J. Ge, L. Zhao, and Y. Tamura, "A new methodology for analysis of static wind loads on super large cooling towers", Journal of Wind Engineering, pp. 30–39, 2012.

[4] El Ansary, "Optimum Shape and Design of Cooling Towers", World Academy of Science, Engineering and Technology, pp 12-21, 2011.

[5] A. W. Rafat, and B.Masud, "Cross winds effect on performance of natural draft wet cooling towers", Journal of Thermal Sciences, pp. 218-224, 2010.

[6] Dr. A. B. Kulkarni, "Analysis of natural draft hyperbolic cooling tower by finite element method using equivalent plate method", International Journal of Engineering Research and Applications, pp.144-148, 2009.

[7] A M Nasir, D P Thambiratnam, D Butler, P Austin, "Dynamics of axisymmetric hyperbolic shell structures", Thin –Walled Structures,Vol. 40,pp.665-690,2002.